Electronic Supplementary Material (ESI) for Chemical Communications

In situ monitoring of the DNA hybridization by attenuated total reflection surface-enhanced infrared absorption spectroscopy

Jian-Yun Xu, Bo Jin, Yun Zhao, Wang Kang*, Xing-Hua Xia*

State Key Laboratory of Analytical Chemistry for Life Science, School of Chemistry and Chemical Engineering, Nanjing University, Nanjing, 210093, China

Fax: +86-25-83685947; Tel: +86-25-83597436; E-mail: wangkang@nju.edu.cn (K. Wang); xhxia@nju.edu.cn (X.H. Xia).

Supporting Information (SI)

Chemicals

All oligonucletides were purchased from Sangon Co., Ltd. (Shanghai, China). The sequences of all oligonucleotides are listed as follows:

Capture DNA (cDNA)： 5′-SH-$(CH_2)_6$-TCG TAC GAT CGA TCC-3′

Target DNA (tDNA)： 5′-GCC GCT CAC ACG ATA TTT TTT TTG GAT CGA TCG TAC GA-3′

Signal DNA (sDNA)： 5′-TAT CGT GTG AGC GGC TTT TTT TT-$(CH_2)_6$-SH-3′

Single-base mismatched DNA (SbmDNA): 5′-GCC GCT CAC ACG ATA TTT TTT TTG GAT CGA TGG TAC GA-3′

Non-complementary DNA (NoncDNA): 5′-ACA TGC TTG GAC TGC TTT TTT TTC AGG CTC ATC GTA CG-3′

4-mercaptobenzoic acid (MBA) and 6-Mercapto-1-hexanol (MCH) were purchased from Sigma-Aldrich. All chemicals if not specified were of analytical grade. All solutions were prepared using ultrapure water (Milli-Q UVplus, Millipore, Inc.; 18.2 MΩ cm^{-1}). UV–vis absorption spectra acquired with a Shimadzu UV-3600 UV/vis spectrophotometer were used to characterize the synthesized AuNPs in order to obtain information about structure and size. The morphology of spherical gold nanoparticles was observed by high resolution transmission electron micrograph (TEM, JEOL-JEM-200CX microscope, Japan) operated at 200 kV. Electrochemical impedance spectroscopy (EIS) measurements were performed on an Autolab electrochemical analyzer (Eco Chemie, The Netherlands) to characterize the assembly and hybridization of DNA on the gold substrate. EIS measurements were performed in a 5 mM $K_3Fe(CN)_6/K_4Fe(CN)_6$ (1:1) mixture with 0.1 M KCl as the supporting electrolyte, and an alternating current voltage of 5.0 mV was applied within the frequency ranging from 0.01 Hz to100 kHz. FT-IR spectra averaged from 128 scans were collected on a Tensor 27 (Bruker Inc., Germany) equipped with a liquid-nitrogen-cooled mercury-cadmium-telluride (MCT) detector.

Synthesis and Modification of Gold Nanoparticles

Citrate-stabilized gold nanoparticles (AuNPs) were prepared through thermal reduction of $HAuCl_4$ by sodium citrate according to the literature.[1] Briefly, 15 mL of 38.8 mM sodium citrate was immediately added to 150 mL of 1.0 mM $HAuCl_4$ refluxing solution under rapid stirring, and kept boiling of the reactant for 15 min. The solution was cooled to room temperature with continuous stirring and then filtered through a 0.2 μm membrane.

TEM imaging of the obtained AuNPs gives an average diameter of 15±3 nm. The TEM images before and after modifying with signal DNA were shown in Figure S1. UV-vis spectra were also used to characterize the change in size of the AuNPs after modifying with signal DNA.

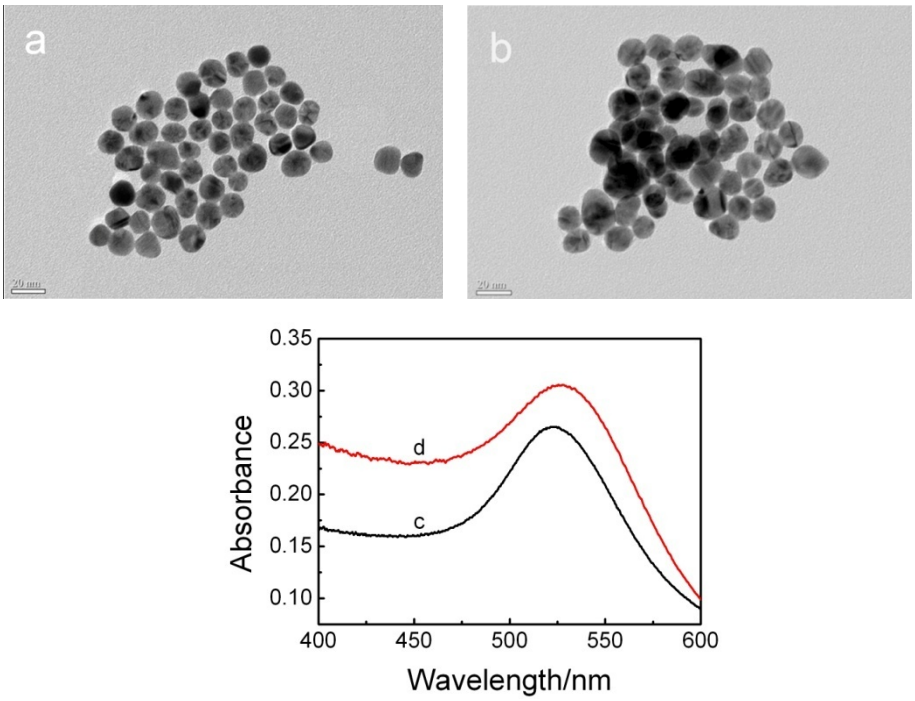

Figure S1. TEM images of the AuNPs solution before (a) and after capture DNA and MBA binding (b); UV-vis spectra of AuNPs solution: (c) naked AuNPs, (d) MBA@AuNPs-sDNA, each of the two curves are the average from two parallel measurements.

The as-prepared 15 nm AuNPs were then comodified with the thiolated signal DNA and MBA.[2] 1 mL of AuNPs suspension (50 nM) was incubated with a mixture of MBA (20 μL, 100 nM) and signal DNA (5 μL, 100 nM) for 16 h at room temperature.

We define the MBA-signal DNA comodified AuNPs as MBA@AuNPs-sDNA. The mixture was slowly brought up to a final salt concentration of 0.15 M NaCl and 50 mM phosphate buffer solution (PBS, pH 7.4) and allowed to age for 40 h. Centrifugation was performed at 10000 rpm for 30 min in order to remove excessive reagents. The precipitate was washed by successive centrifugation-suspension steps in the above PBS solution for three times and finally dispersed in 50 mM PBS (pH 7.4) containing 0.15 M NaCl for further use.

EIS Characterization of the DNA Assembly and Hybridization

Figure S2 shows Nyquist plots of impedance for stepwise assembly of Au substrates. The increase of interfacial electron transfer resistance (R_{ct}) is due to the immobilization of negatively charged probes on the recognition interface resulting in a negatively charged interface which electrostatically repels the negatively charged redox probe $[Fe(CN)_6]^{3-/4-}$ and inhibits interfacial charge-transfer.[3] The observed increase of R_{ct} indicates a successfully stepwise and uniform assembling process.

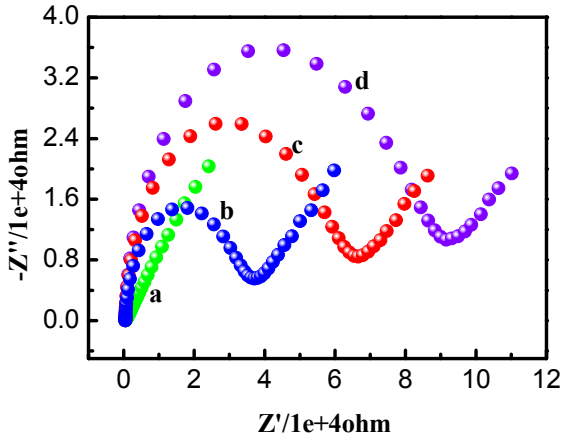

Figure S2. Nyquist plots in PBS buffer (10 mM, pH 7.4) containing 5 mM $Fe(CN)_6^{3-/4-}$ at 210 mV for (a) a bare gold substrate, (b) the thiolated cDNA modified gold substrate, (c) the obtained (b) hybridization with 100 nM target DNA, (d) the obtained (c) after hybridization with 100 nM target DNA and MBA@AuNPs-sDNA. Frequency range: 0.1-100 kHz; ac amplitude, 5 mV.

Comparison of the IR Spectra of MBA Powder and the MBA in Sandwich Hybridization Structure

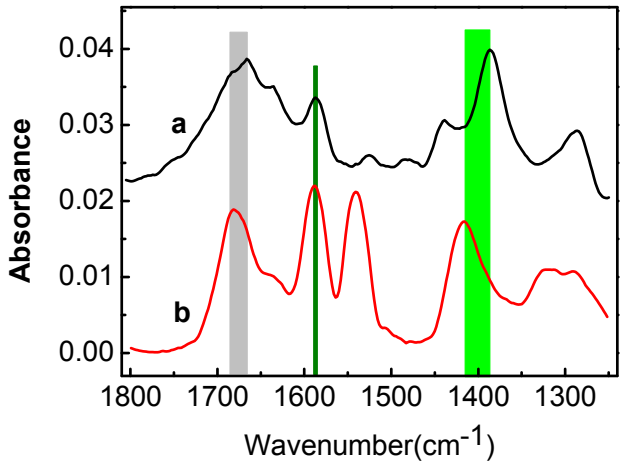

Figure S3. Comparison of the IR spectra of MBA in MBA@AuNPs-sDNA sandwich hybridization structure (a) and MBA powder (b).

From Figure S3 we just observed the C=O stretching band tiny red shift from 1680 cm-1 to 1666 cm-1. The isoelectric point of MBA is 4.79, besides; the pH value of the buffer solution is 7.4. We consider MBA is in the state of deprotonated. On deprotonation, $\nu_{C=O}$ shifts to lower energy as its vibrational mode becomes coupled to that of the other oxygen, giving rise to a shift from 1680 to 1666 corresponding to changing the carboxyl group into carboxylate with a change in its bong arrangement into one and half linkage.

Reproducibility of the SEIRAS System for the Measurement of DNA Hybridization Kinetics

Figure S4 shows the surface enhanced infrared absorption spectra of DNA hybridization from five arrays to further evaluate the repeatability of this method and focuses on the two dominant modes of the probe molecules MBA which are at 1666 cm^{-1} and 1587 cm^{-1}. Hybridization was allowed to proceed for 8 h at room temperature, which ensures that different hybridization efficiency and hybridization kinetics based on different tests can be observed.

The results were analyzed and treated using normalization Figure S4a. The curves of Figure S4a do, however, conform at least approximately to an exponential, as expected for a first-order process. Using a highly simplified model of the

hybridization process, we can determine the rate constant of DNA hybridization. If we assume a first-order binding process, then the rate constant can be obtained from a logarithmic plot of band intensity against time (Figure S4b). In Figure S4b, the corrected band intensity in fact responds to the relative amount of target DNA at any moment or at long times. Linear fitting to the data (solid lines) yields the rate constant, k for hybridization.

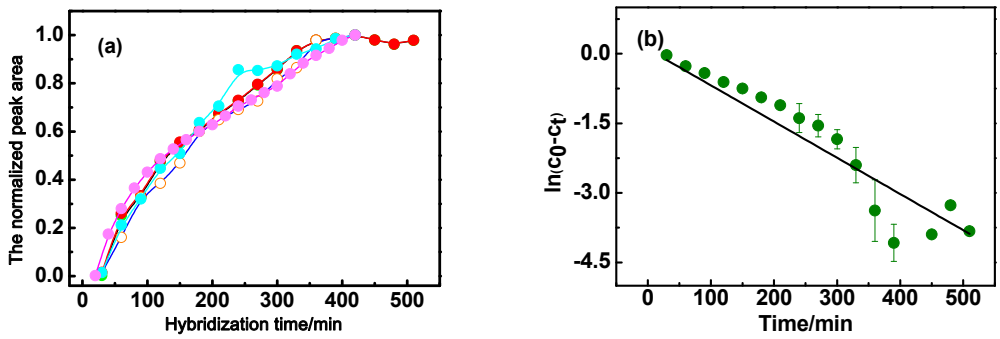

Figure S4. Dynamic curves of DNA hybridization obtained by comparison of the relative intensities of IR bands at 1666 cm^{-1} and 1587 cm^{-1} with 200 nM of target DNA at room temperature (a); mathematical model of hybridization kinetics (b).

DNA Self-Assembly and Hybridization ona Gold Film Modified Si Prism Surface

The prepared Au film has an island structure with SEIRAS-activity (Figure S5). Self-assembly of capture DNA on the Au film was accomplished by incubating the substrate in a solution consisting of 100 nM capture DNA at room temperature for 24 h. Then, the Au surface was washed with water for 30 s to remove nonspecifically bound DNA probes. The capture DNA-modified gold film was dipped in 1 mM MCH solution for 30 min at room temperature. This step of ligand exchange reaction removed nonspecifically adsorbed and some of the chemically attached DNA from the Au film surface, which improved subsequent biomolecular recognition (e.g., hybridization) efficiency.[4, 5] In the hybridization step, the surface was let in contact with 100 nM target DNA for 2 h. Then, the hybridized surface was extensively rinsed with buffer solution. The MBA@AuNPs-sDNA was then added to hybridize with the overhanging region of the target sequence. Subsequently, nonspecifically bound

nanoparticles were extensively washed off with buffer (0.15 M NaCl, 50 mM phosphate buffer solution, pH 7.4).

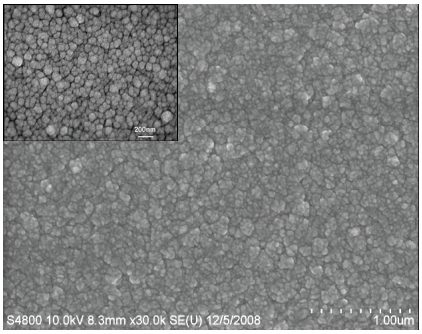

Figure S5. SEM image of gold nanofilm deposited on a silicon optical prism surface.

ATR-SEIRAS Detection of DNA Hybridization

Our experiments were carried out with an apparatus consisting of a Fourier transform infrared (FTIR) spectrometer (Bruker TENSOR 27 with a liquid nitrogen cooled MCT detector). The spectral window was 4000-400 cm^{-1} with a nominal spectral resolution of 4 cm^{-1}. The prism used was a non-doped Si(111) hemicylinder with a diameter of 30 mm (ALKOR Technologies Co., Russia). The reflecting plane of the prism was the interface between the Si and deposited Au film. All spectra were shown in the absorbance units. The kinetics of DNA hybridization was studied using homemade ATR-SEIRAS setup. Deposition of gold film on the silicon surface has been described in detail previously. Such technique need to record a baseline before further measurement. Therefore, the surface was first immersed in pure buffer for 20 min to get the baseline. Then all the other IR adsorption curves are recorded relative to this baseline. The O-H stretching of water is automatically subtracted by the IR software.

Table S1. The SEIRAS peak frequency assignments

Peak position	Assignment	Designation
1666 cm^{-1}	C=O stretch [6]	υ (CO-)
1636 cm^{-1}	COO^- asymmetric stretch [7]	$\upsilon_a(CO_2\text{-})$
1587,1525,1484 cm^{-1}	C=C aromatic stretch [8,9]	$\upsilon_{ring}(C=C)$
1542 cm^{-1}	COO-(asymmetric stretch) [10]	$\upsilon_a(CO_2\text{-})$

1439 cm^{-1}	C-H bend [11]	δ(C-H)
1386 cm^{-1}	COO-symmetric stretching [12,13]	$\upsilon_s(CO_2^-)$
1286 cm^{-1}	C-O stretch [7]	υ(C-O)
1311 cm^{-1}	C-OH strctch/ C-O-H bend [14]	υ(C-OH), δ(C-O-H)

δ = bend or deformation; υ = stretch; ring = ring breathing mode; a = antisymmetric; s = symmetric

(1) Grabar, K. C.; GrWith Freeman, R.; Hommer, M. B.; Natan, M. J. *Anal. Chem.* **1995**, *67(4)*, 735–743

(2) Zhu, Z. Q.; Su, Y. Y.; Li, J.; Li, D.; Zhang, J.; Song, S. P.; Zhao, Y.; Li, G. X.; Fan, C. H. *Anal. Chem.* **2009**, *81(18)*, 7660–7666

(3) Zhang, S. S.; Xia, J. P.; Li，X. M. *Anal. Chem.* **2008**, *80(22)*, 8382–8388

(4) Zhao, W.; Chiuman, W.; Lam, J. C. F.; McManus, S. A.; Chen, W.; Cui, Y. G.; Pelton, R.; Brook, M. A.; Li, Y. F. *J. Am. Chem. Soc.* **2008**, *130(11)*, 3610–3618

(5) Peng, H. I.; Strohsahl, C. M.; Leach, K. E.; Krauss, T. D.; Miller, B. L. *ACS Nano* **2009**, *3(8)*, 2265–2273

(6) Kaake, L. G.; Zou, Y.; Panzer, M. J.; Frisbie, C. D.; Zhu, X. Y. *J. Am. Chem. Soc.* **2007**, *129(25)*, 7824–7830

(7) Dibbell, R. S.; Youker, D. G.; Watson, D. F. *J. Phys. Chem. C* **2009**, *113(43)*, 18643–18651

(8) Hao, E.; Lian, T. Q. *Langmuir* **2000**, *16(21)*, 7879–7881

(9) Smith, E. L.; Alves, C. A.; Anderegg, J. W.; Porter, M. D.; Siperko, L. M. *Langmuir* **1992**, *8(11)*, 2707–2714

(10) Rosendahl, S. M.; Burgess, I. J. *Electrochimica Acta* **2008**, *53(23)*, 6759–6767

(11) Banerjee, S.; Wong, S. S. *Nano Lett.* **2002**, *2(3)*, 195–200

(12) Chen, T.; Wang, H.; Chen, G.; Wang, Y.; Feng, Y. H.; Teo, W. S.; Wu, T.; Chen, H. Y. *ACS Nano* **2010**, *4(6)*, 3087–3094

(13) Orendorff, C. J.; Gole, A.; Sau, T. K.; Murphy, C. J. *Anal. Chem.* **2005**, *77(10)*, 3261–3266

(14) Creager, S. E.; Steiger, C. M. *Langmuir* **1995**, *11(6)*, 1852–1854